

Beyond boundaries: pioneering discoveries in aldose reductase inhibition for diabetic neuropathy

Original Article

Abstract:

Aldose reductase enzyme is involved in key step controlling the polyol pathway and acknowledged as a possible target for diabetic neuropathy. The anionic region of the active site comprising residues His110 and Tyr48 is involved in the detoxification mechanism that is considered important. This process involves eliminating toxicity through conversion of aldehydes such as methylglyoxal (MeG) and 3-deoxyglucosone. So far, no drug has been developed that could selectively inhibit reduction of glucose to sorbitol without affecting the detoxification mechanism. To comprehend the critical interactions of the known aldose reductase inhibitors and the enzyme, molecular docking was conducted in this study. Anionic region, specificity region and the active site are the three regions used separately for grid molecular docking studies to identify the possible inhibitors that selectively bind to specificity region. Among the docked compounds, quercetin was found to bind to specificity region, so we chose reported quercetin analogue and built a pharmacophore model. Subsequently, a collection of 82,000 natural substances from the IBS databank (InterBioScreen) was searched using a 6-point pharmacophore (AAARRR) that was created. After the initial search returned 2,394 hits, a hierarchical docking approach was used to identify an intriguing hit molecule (mol_7921), which is quite close to a flavonoid compound. Molecular dynamics simulation was used to confirm the hit molecule-aldose reductase complex's structural stability. For its possible inhibitory effect, this molecule could be tested and used to treat diabetic neuropathy.

Key words:

diabetic neuropathy, polyol pathway, methylglyoxal, quercetin, virtual screening, inhibitors

Apstrakt:

Iza granica: Pionirska otkrića u inhibiciji aldoza reduktaze za dijabetičku neuropatiju

Enzim aldoza reduktaza je uključen u ključni korak kontrole poliolskog puta i prepoznat je kao moguća meta za dijabetičku neuropatiju. Anjonski region aktivnog mesta, koji obuhvata ostatke His110 i Tyr48, uključen je u mehanizam detoksikacije koji se smatra važnim. Ovaj proces podrazumeva eliminaciju toksičnosti kroz konverziju aldehida, kao što su metil glioksal (MeG) i 3-dezoksiglukoza. Do sada nije razvijen nijedan lek koji bi mogao selektivno inhibirati redukciju glukoze u sorbitol bez uticaja na mehanizam detoksikacije. Kako bismo razumeli ključne interakcije poznatih inhibitora aldoza reduktaze i enzima, sprovedeno je molekularno dokovanje u ovoj studiji. Anjonska regija, specifična regija i aktivno mesto su tri regije korišćene zasebno za dokovanje molekula kako bi se identifikovali mogući inhibitori koji se selektivno vezuju za specifičnu regiju. Među dokovanim jedinjenjima, ustanovljeno je da se kvercetin vezuje za specifičnu regiju, pa smo odabrali prijavljeni analog kvercetina i izgradili farmakoforski model. Nakon toga, pretraženo je 82.000 prirodnih supstanci iz IBS baze podataka (InterBioScreen) koristeći farmakofor sa 6 tačaka (AAARRR). Početna pretraga vratila je 2.394 pogodaka, nakon čega je korišćen hijerarhijski pristup dokovanju kako bi se identifikovalo ciljno jedinjenje (mol_7921), koje je veoma blisko flavonoidnom jedinjenju. Simulacija molekulske dinamike je korišćena da potvrdi strukturu stabilnosti kompleksa ciljnog molekula i aldoza reduktaze. Ovo jedinjenje bi moglo biti testirano i korišćeno za lečenje dijabetičke neuropatije zbog svog mogućeg inhibitorynog efekta.

Ključne reči:

dijabetička neuropatija, put poliola, metil glioksal, kvercetin, virtualni skrining, inhibitori

Nagarajan A.

Department of Pharmaceutical Chemistry,
Karpagam College of Pharmacy, Coimbatore –
641032, Tamilnadu, India; The Tamil Nadu Dr.
M.G.R. Medical University, Chennai – 600032,
Tamilnadu, India
nagarajan.a@kcp.edu.in (corresponding author)
<https://orcid.org/0000-0002-6845-934X>

Vignesh C.

Department of Biotechnology, Sastra University,
Thanjavur, Tamilnadu, India

Ramasamy T.

Department of Biotechnology, Ennam College of
Pharmacy, Kinathukadavu Taluk, Coimbatore –
641032 Coimbatore – 641032, Tamilnadu, India

Sasikala M.

Department of Pharmaceutical Analysis, Karpagam
College of Pharmacy, Coimbatore – 641032, Tamil-
nadu, India; The Tamil Nadu Dr. M.G.R. Medical
University, Chennai – 600032, Tamilnadu, India

Mohan S.

Department of Pharmaceutics, Karpagam College of
Pharmacy, Coimbatore – 641032, Tamilnadu, India;
The Tamil Nadu Dr. M.G.R. Medical University,
Chennai – 600032, Tamilnadu, India

Received: August 27, 2024

Revised: September 25, 2024

Accepted: September 30, 2024



Introduction

Diabetic neuropathy is a complication of diabetes attributed to the failure of peripheral nerves and reduction in myelinated nerve fiber density. Diabetes treatment using herbal medicine has been explored and natural flavonoids such as quercetin find use in treating diabetes, as revealed by several studies (Yagihashi et al., 2011; Madić et al., 2017; Jensen et al., 2021). It also depicts other symptoms such as nerve pinch, prolonged pain and loss of sensitivity (Gronda et al., 2020). This disorder strikes the peripheral nerves that are present outside the brain, at the terminals of the spinal cord. They disrupt the nerve conduction mechanism in these peripheral nerves. In fact, the prevalence of diabetic neuropathy is 7% in the first year of diagnosis reaching up to 50% for those with more than 25 years (Singh et al., 2021). Loss of sensation in the lower limbs causes limb amputation in 1–2% of diabetic patients and requires high cost of treatment. Making an early diagnosis and managing diabetic neuropathy are challenging, and currently, no cure is available.

The polyol pathway converts glucose to sorbitol by reduction through enzyme aldose reductase which is the key factor behind this complication of diabetes. Aldehyde reductase comes under the family of oxidoreductases. Under normal conditions, aldose reductase enzyme doesn't show significant affinity in binding to glucose. On the other hand, under high blood sugar conditions, the amount of glucose retained in the system without being converted into energy increases. Such left out volumes of glucose easily pass through the membranes of nerve cells, kidney cells and retinal cells. After entrance, they bind to aldose reductase, as it has a higher affinity for them under such conditions (Twarda-Clapa et al., 2022). This doesn't mean that the normal energy conversion process won't take place, but the glucose being released in larger volumes cannot be incorporated into the normal process of energy conversion and moves into the next possible process, here being the polyol pathway. Diabetic neuropathy is a complication associated with diabetes caused by an increase in glucose flux under hyperglycemic conditions leading to the accumulation of sorbitol in nerve cells (Goto et al., 1995). This causes reduced myo-inositol production (Goto et al., 1995) in addition to inducing the production of advanced glycation end products (AGE's). The anionic region of the active site has residues His110 and Tyr48 that are involved in the much important detoxification mechanism (Klebe et al., 2004) wherein methylglyoxal and 3-deoxyglucosone are reduced to curb toxicity. Several aldose reductase inhibitors (ARI) emerged, but not successful at clinical owing to the adverse

effects or inferior efficacies. Epalrestat, licensed in Japan is the single drug of this category (Kumar et al., 2012).

Aldose reductase carries out a process of detoxifying the toxic aldehydes. All the synthetic and natural inhibitors studied so far interfere with the detoxification mechanism by occupying that region or binding to residues Trp111, His110, and Tyr48 (Imran et al., 2022). This inner anionic region of the active site generally carries out this process of detoxification by binding to toxic aldehydes (Sulaiman et al., 2022). When this process is affected, toxic aldehydes in the system glycate the nitrogen on collagen-like proteins, forming AGEs, which contribute to diabetic complications such as peripheral neuropathy, diabetic nephropathy, and diabetic angiopathy. Therefore, finding a drug that would focus on selective inhibition of aldose reductase binding to glucose without affecting the detoxification mechanism would prove a good solution.

The detoxification mechanism is a vital phenomenon that takes place with the assistance of aldose reductase enzyme, where the toxic aldehydes come and bind to the residues Trp111, His 110, Tyr48 present in the inner anionic region of the active site. Glucose generally comes in and binds to the active site making interactions with Tyr48 that donates a proton during the reduction mechanism (Chen et al., 2022). Therefore, finding an inhibitor that would block the entry of glucose (a bulkier group) while allowing toxic aldehydes, such as methylglyoxal and 3-deoxyglucosone (three-carbon group compounds), to enter the pocket helps us eliminate the reduction of glucose to sorbitol and does not affect the detoxification mechanism.

Sulaiman et al. (2022) reported the presence of markers related to antioxidant property and carbonic anhydrase level in correlation with diabetes complications (Chen et al., 2022). Advanced glycation end products were related to molecular mechanisms underlying the skin fibroblast growth parameters (Cicccone et al., 2022). Antioxidant utility in combination with aldose reductase inhibition has been evaluated with several benzaldoxime derivatives (Zhang et al., 2022). The potential of aldose reductase inhibitory activity has been suggested to improve treating injury of medulla spinalis through neuronal differentiation of transplanted NSCs (Zheng et al., 2021). Emodin has been evaluated as a potential candidate for treating metabolic diseases through its multifaceted role in inflammation and diabetes (Saeed et al., 2022). These authors have identified 6-oxo-6,9-dihydro-1H-purin-8-yl) thio) acetamide as potential aldose reductase inhibitor through pharmacophore-based

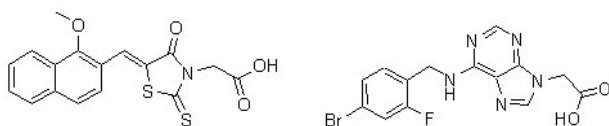


Fig. 1. Structures of known aldose reductase inhibitors (Z)-2-(5-((1-methoxynaphthalen-2-yl)methylene)-4-oxo-2-thioxothiazolidin-3-yl)acetic acid, 2-(6-((4-bromo-2-fluorobenzyl)amino)-9H-purin-9-yl)acetic acid (Zhu et al., 2022)

search in NuBBE_{DB} database (Bakal et al., 2022). Using molecular simulation and docking Bakal et al. (2022) identified (Z)-2-(5-((1-methoxynaphthalen-2-yl)methylene)-4-oxo-2-thioxothiazolidin-3-yl)acetic acid derivative as aldose reductase inhibitor (**Fig. 1**). Recent reports on the identification of thiazolidin-dione through docking showed interactions with residues Trp111, Ala299, Leu300 and Phe122 located at the specificity pocket (Balestri et al., 2022), and reviewed various natural and synthetic compounds that act as aldose reductase inhibitors, including cyclic imides, polyphenols, and carboxylic acid derivatives (Friesner et al., 2006; Zhu et al., 2022). Zhu et al. (2022) revealed the purine derivatives (**Fig. 1**) as a potential inhibitor of aldose reductase having an IC₅₀ value of 0.038 μM. These reports suggest that there is still no selective inhibitor for aldose reductase warranting further search for a candidate molecule to address the diabetic complication affecting the eye.

Materials and Methods

Overview of steps used in the present study is given in **Fig. 2**. An initial docking analysis was carried out with set of natural compounds that were tested *in vitro* for inhibition of aldose reductase. We

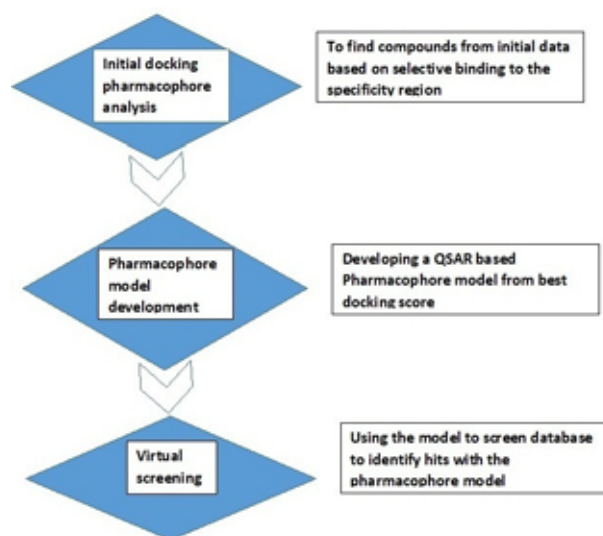


Fig. 2. Steps used in identification of hits

understood the pharmacophore requirements using the same set of compounds that were likely to bind to the target region i.e. the specificity region of our enzyme active site. Then a pharmacophore model was developed using a set of analogues from the most likely compound that could be considered as a starting point for finding a perfect inhibitor. A 3D database search was carried out using the obtained pharmacophore model and a final docking analysis was carried out using the hits from the search to screen out fewer effective compounds. *In silico* tools such as virtual library screening, docking methods, LigPrep, protein preparation and pharmacophore analysis were carried out using the GUI Maestro v9.1 of the Schrödinger software (Rajeswari et al., 2014). PHASE module of Schrödinger software was used to build a six-point pharmacophore (Verma & Thareja, 2020).

Data set

Ligands for Initial Analysis

The initial set of natural and synthetic ligands were obtained from different literature and deposited PDB structures, respectively. We collected diverse natural compounds (Chaudhry et al., 1983) that have been found effective *in vitro*. Ligands from co-crystallized PDB structures were obtained to confirm the reliability of our results from the initial docking analysis. Also, methylglyoxal structure was obtained to confirm its binding to the anionic region of the binding pocket.

The set of natural and synthetic compounds as described earlier were created using SYMYX Draw v4.0. They were prepared using LIGPREP module of the GUI Maestro v9.1. Docking was employed with extra-precision mode (XP mode) of GLIDE software of the GUI Maestro v9.1.

Receptor Protein

The receptor protein was retrieved using the Protein Data Bank which is a depository of protein structures. The structure of aldose reductase bound to two molecules of benzothiazepine inhibitor (PDB id: 3P2V) at the resolution of 1.69 Å was chosen as the receptor for all further studies (**Fig. 3**). This is the structure of aldose reductase which is a 316aa long and co-crystallized with two benzothiazepine inhibitors in its active site. The compounds with structure shown in **Fig. 4** are taken for preliminary screening.

Results

In our work, we docked methylglyoxal (a toxic aldehyde) and found it occupying the exact same anionic region. Therefore, we used the docked

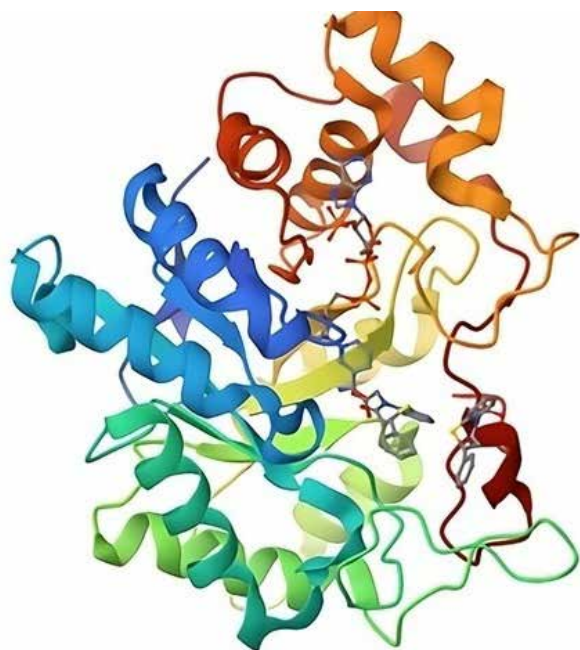


Fig. 3. Structure of aldose reductase bound to novel benzothiazepine PDB id: 3P2V

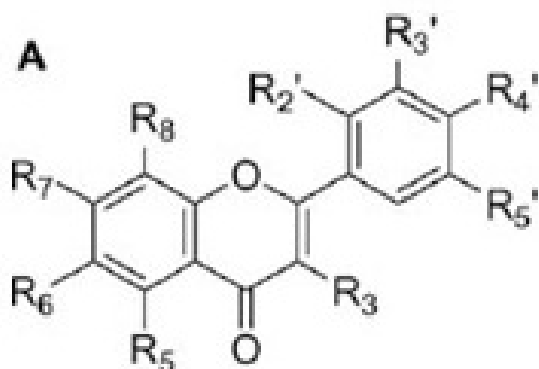


Fig. 4. The quercetin scaffold used to derive analogues for pharmacophore model development

receptor-ligand complex for further docking analysis with the set of natural and synthetic compounds. Grids were prepared for the anionic region, important region and the active packet separately (**Fig. 5**). Quercetin analogues (**Fig. 6, Tab. 1**) with *in vitro* activity (Kondhare et al., 2017) were used to build a QSAR-based pharmacophore model and utilized this model to screen a library of natural compounds (82,000) obtained from IBS database in search of a selective inhibitor. These authors have compared the activity and stated that “improvement observed in the inhibition of glycosylated sugar myricitrin was higher than that observed for the aglycone myricetin (Kondhare et al., 2017).

The specificity pocket forms the entry part of the active site at the external surface. The docking

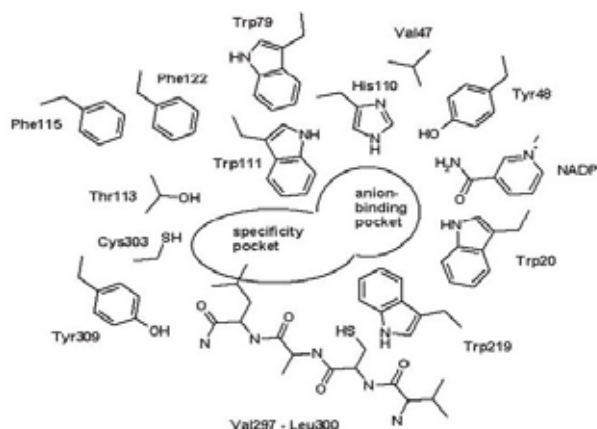


Fig. 5. The active site residues making up the two regions

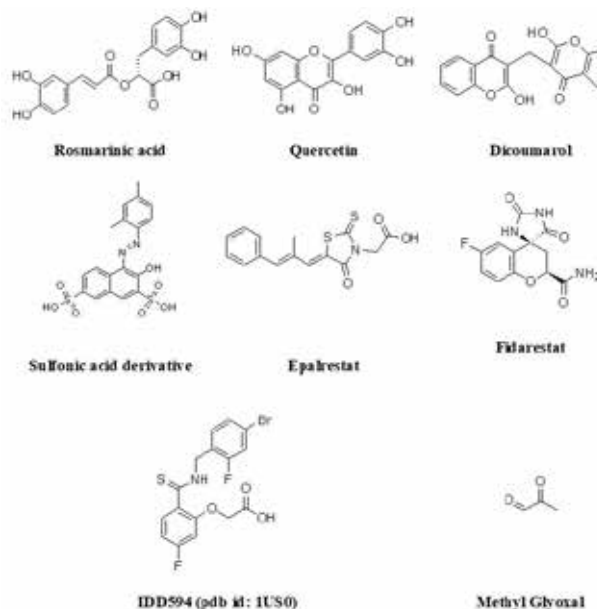


Fig. 6. Structures chosen for initial docking study

analysis was carried out by setting grids for anion binding, region specific to binding and the active regio as a whole and the same set of compounds were docked into these three regions. The obtained results are presented in **Tab. 2**.

The reliability of this analysis was confirmed by the observations made with respect to the binding of the toxic aldehyde, methylglyoxal. Methylglyoxal docked with the residues Trp111, His110 and Tyr48 of anionic region showed interaction which reflected the literature studies explaining the detoxification mechanism. Also, the ligands obtained from PDB structures docked into the active site, making 80% of the interactions as in the deposited structures. In the case of rosmarinic acid, although it showed good interactions and better docking scores, its size and

Table 1. Quercetin analogues and their activity values

| S. No. | Scaffold | Substituent | Activity [log(1/IC ₅₀)] µM | S. No. | Scaffold | Substituent | Activity [log(1/IC ₅₀)] µM |
|--------|----------|---|--|--------|----------|--|--|
| 1 | A | 5, 7, 3', 4'-OH; 3,6-OCH ₃ | 7.59 | 26 | A | 5,6,3',4'-OH; 7-OCH ₃ | 6.52 |
| 2 | A | 3',4'-OH; 5,6,7,8-OCH ₃ | 7.49 | 27 | A | 6,3',4'-OH; 3,5,7-OCH ₃ | 6.52 |
| 3 | A | 6,3',4'-OH; 5,7,8-OCH ₃ | 7.44 | 28 | A | 5,3',4'-OH; 3,6,7-OCH ₃ | 6.46 |
| 4 | A | 5,7,3',4'-OH; 6-OCH ₃ ; 8-CH ₂ Ph | 7.47 | 29 | A | 5,7,4'-OH; 6,8-OCH ₃ | 6.39 |
| 5 | A | 5,3',4'-OH; 6,7,8-OCH ₃ | 7.41 | 30 | A | 5,4'-OH; 6,7,8-OCH ₃ | 6.27 |
| 6 | A | 3',4'-OH; 5,7,8-OCH ₃ | 7.35 | 31 | A | 5,6,3',4'-OH; 3,7-OCH ₃ | 6.09 |
| 7 | A | 5,6,7,3',4'-OH; 3-OCH ₃ | 7.24 | 32 | A | 3,5,7,3',4'-OH | 6.02 |
| 8 | A | 5,6,3',4'-OH; 7,8-OCH ₃ | 7.19 | 33 | A | 5,6,4'-OH; 7,8-OCH ₃ | 6.07 |
| 9 | A | 7,3',4'-OH; 5,8-OCH ₃ | 7.13 | 34 | A | 5,6,7,4'-OH; 8-OCH ₃ | 5.92 |
| 10 | A | 5,3',4'-OH; 7,8-OCH ₃ | 7.11 | 35 | A | 5,6,7,4'-OH; 8,3'-OCH ₃ | 5.92 |
| 11 | A | 3,4'-OH; 5,6,7-OCH ₃ | 7.04 | 36 | A | 5,4'-OH; 6,7-OCH ₃ | 5.85 |
| 12 | A | 5,6,7,3',4'-OH; 8-OCH ₃ | 6.92 | 37 | A | 5,7,3',4'-OH; 3-O-Rh | 6.54 |
| 13 | A | 6,3',4'-OH; 5,7-OCH ₃ | 6.85 | 38 | A | 5,7,4'-OH; 6,8,3'-OCH ₃ | 5.35 |
| 14 | A | 4'-OH; 5,6,7,8-OCH ₃ | 6.79 | 39 | A | 6,4'-OH; 5,7,8,3'-OCH ₃ | 5.2 |
| 15 | A | 8,3',4'-OH; 5,7-OCH ₃ | 6.79 | 40 | A | 5,4'-OH; 6,7,3'-OCH ₃ | 5.17 |
| 16 | A | 3',4'-OH; 3,5,7,8-OCH ₃ | 6.77 | 41 | A | 5,7-OH; 6,8,4'-OCH ₃ | 5.14 |
| 17 | A | 5,6,7,3',4'-OH | 6.69 | 42 | A | 5,6,7-OH; 8-OCH ₃ | 5.09 |
| 18 | A | 5,3',4'-OH; 6,7-OCH ₃ | 6.92 | 43 | A | 5,6-OH; 7,8-OCH ₃ | 5.08 |
| 19 | A | 5,8,3',4'-OH; 7-OCH ₃ | 6.64 | 44 | A | 3',4'-OH; 5,6,7-OCH ₃ ; 3-COCH ₃ | 5.05 |
| 20 | A | 5,7,3',4'-OH; 3,8-OCH ₃ | 6.62 | 45 | A | 5,3'-OH; 6,7-OCH ₃ ; 4'-O-Glc | 5.09 |
| 21 | A | 6,4'-OH; 5,7,8-OCH ₃ | 6.6 | 46 | A | 5-OH; 6,7,3'-OCH ₃ ; 4'-O-Glc | 4.6 |
| 22 | A | 3',4'-OH; 5,6,7-OCH ₃ | 6.57 | 47 | A | 5-OH; 6,7-OCH ₃ ; 4'-O-Glc | 4.6 |
| 23 | A | 5,7,3',4'-OH; 8-OCH ₃ | 6.55 | 48 | A | 5,7-OH; 6,8,3'-OCH ₃ ; 4'-O-Glc | 4.33 |
| 24 | A | 7,3',4'-OH; 3,5,8-OCH ₃ | 6.55 | 49 | A | 4'-OH; 5,6,7,8,3'-OCH ₃ | 4.74 |
| 25 | A | 8-OCH ₃ ; 5,6,7,3',4'-OCOCH ₃ | 6.52 | 50 | A | 5,4'-OH; 6,8,3'-OCH ₃ ; 7-O-Glc | 4.15 |

Table 2. Quercetin analogues and their activity values

| Compound | Interactions when docked into the specificity pocket (docking score) | Interactions when docked into the anionic region | Interactions when docked into the active site | Selectivity towards |
|--------------------------|--|--|---|---------------------|
| Bis-coumarin | Leu300 [-11.74] | Leu300 [-12.62] | Trp111 [-11.10] | Intermediate |
| Epalrestat | Ala299, Leu300 [-12.303] | Tyr48, His110, Trp111 [-11.07] | Trp111 [-11.10] | Both regions |
| Sulfonic acid derivative | Leu301, Ser302, Trp111 [-11.04] | Trp111, Tyr48 [-11.23] | Ala299, Leu300, Leu301, Trp111 [-6.684] | Both |
| Quercetin | Leu300, Leu301 [-12.981] | Leu300, Leu301 [-12.719] | Ala299, Leu301, His110 [-13.293] | Specificity region |
| Rosmarinic acid | Ser302(2), Leu300, Lys221 [-12.37] | Val47, Tyr48, His110, Trp111, Ala299 [-14.904] | Ala299, Leu301, NADP, His110 [-17.05] | Both regions |
| Fidarestat | Trp111, Leu300 [-10.19] | Trp20, Trp111, NADP [-10.10] | Leu300, Trp111, His110, Tyr48 [-10.45] | Both regions |
| IDD594 | Ala299, Leu300, Trp111 [-11.11] | Trp111, NADP, Tyr48 [-13.13] | Trp111, His110, Tyr48 [-6.457] | Both regions |
| Methylglyoxal (MeG) | Trp111, His110 [-6.309] | Trp111, Tyr48, His110 [-6.341] | Trp111, His110, Tyr48 [-6.317] | Both regions |

* glide scores are enclosed in square brackets

the volume that it occupies represented a drawback. As a part of the analysis for this process, we found quercetin selectively occupying the specificity pocket in all the three cases of docking (except for one case where it made interaction with the His110 when docked into the active site as a whole). Quercetin, a natural ligand found in citrus fruits, has been identified as a potent inhibitor in various *in vitro* studies. However, it has exhibited some side effects, which have prevented its acceptance as a drug. Therefore, with these observations we took over quercetin and proceeded for the next step of developing a pharmacophore model based on quercetin analogues.

Pharmacophore Feature Analysis

We considered the compounds that docked into the specificity region and studied their pharmacophore features to understand the groups required for effective binding into that region. The compounds chosen were rosmarinic acid, sulfonic acid derivative, bis-coumarin, quercetin, fidarestat and IDD594 (Fig. 6).

The ligands were prepared, and its conformers were generated as a part of the process. They were

cleaned later to rule out bad, duplicated structures. Respective activity values were specified and based

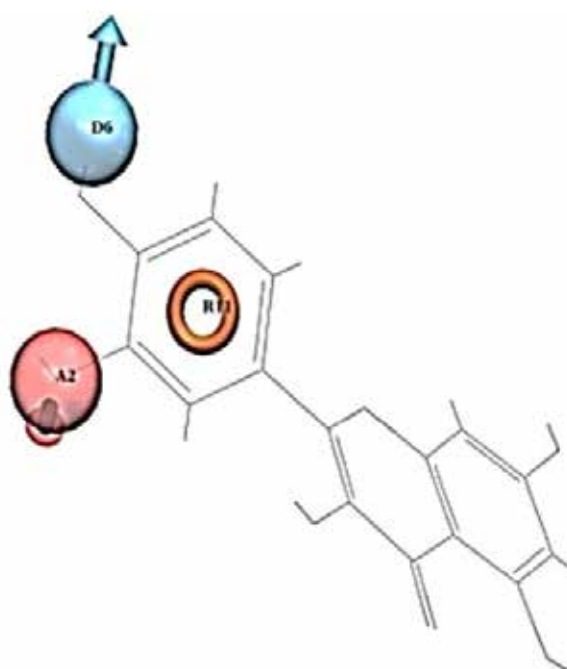


Fig. 7. ADR features mapped over quercetin

on the maximum hypothesis generated; a 3-point pharmacophore (**Fig. 7**) was obtained with ADR (acceptor, donor and ring) features.

This provided us with an understanding that for a molecule to bind into the specificity region, it must have at least two of these three or a combination of such features. Since our specificity comprises the residues Ala299 and Leu300-301, which possess hydrogen bond donor/acceptor functionalities, it facilitates interactions that form hydrogen bonds with incoming ligand molecules. Provided that the ligand is appropriately sized, it will engage exclusively with the specificity region and will not intrude into the anionic region of the active site. Although sulfonic acid derivative showed good fitness (3.000) and a better alignment score (0.000) than quercetin, it does not satisfy the necessary criteria and was found extending into the anionic region during the initial docking analysis. Also, quercetin comparatively had better fitness (2.328) and a good alignment score (0.033). The size and the volume it occupies places quercetin ahead of sulfonic acid derivative to be taken for further studies. The specificity pocket has the property of adapting different inhibitors since the residues 297-300 show adaptations with respect to the inhibitor binding to it. As a smaller molecule than the sulfonic acid derivative, quercetin can create space for toxic aldehydes to enter upon binding. In contrast, the sulfonic acid derivative fits perfectly at the entry of the active site, preventing additional compounds from accessing this space.

Pharmacophore Model Development

Quercetin analogues were designed as described earlier in **Tab. 1** using SYMYX Draw v4.0. These ligands were generated with LIGPREP of the Maestro v9.1 GUI interface. Conformers were generated and their geometries were cleaned accordingly to rule out bad as well as duplicate structures. Activity values (pIC_{50}) were specified to separate out the active from the inactive molecules. With quercetin in mind, a 6-point pharmacophore model was developed,

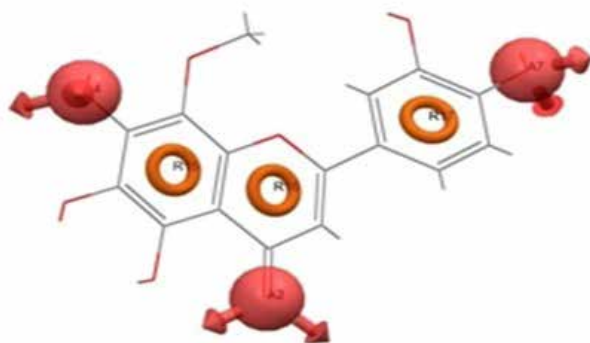


Fig. 8. Model AAARRR (Best fit - A12)

achieving the highest score for this hypothesis. The model (**Fig. 8**) had the features AAARRR (3 H-bond acceptors and 3 aromatic characteristics).

The three ring features aligned with the core structure of a flavonoid. In our case, quercetin, the obtained model provides better chance for searching an optimum compound with the 6 features since it could result in finding a molecule which will have a smaller size and could make hydrogen bonds with the specificity pocket easily. This will help us finding a molecule with a similar core structure (3 ring structures) which is important for our study such that the functional groups would bind accordingly to the residues in the specificity region rather than entering the anionic region.

Virtual Screening

The 6-point pharmacophore (AAARRR) was used as the basis for search from a library of natural compounds obtained from IBS database (InterBioScreen). A total of 82,000 compounds were taken from the database and a pharmacophore-based search was carried out. 2394 hits were obtained as a result of the initial search. These hits were stored as a separate entry and prepared using LIGPREP module of the GUI Maestro v9.1. LIGPREP helps in generating conformers and unique geometries. After preparation we had 5745 entries in hand. We proceeded with a stepwise docking-based screening process to screen out compounds and retain the best ones. The three stages included HTVS Docking, SP Docking and XP docking. In high throughput virtual screening docking, the criteria were set to retain only 5% of the best posed molecule conformations. This brought down the number of hits to 287. In standard precision docking, the criteria were set to retain 10% of the best posed molecule conformations. Thus, we ended up with 28 compounds for the final screening procedure. Using Extra Precision docking, we initially selected the top 14 hits from the SP docking based on their scores and retained the best pose from this step. Consequently, we identified a specific hit that docked as anticipated in the entry region of the specificity pocket. The final hit, mol_7921, exhibited a core structure similar to that of quercetin (**Fig. 9**).

It occupied the specificity pocket making strong hydrogen bond interaction with residues Val297, Ala299, Leu300 (**Fig. 10A** and **Fig. 10B**) had a score

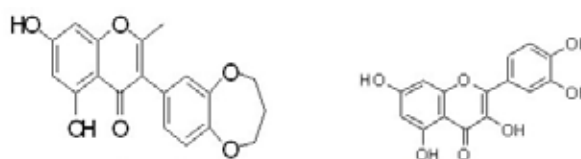


Fig. 9. Final hit (left) compared with quercetin

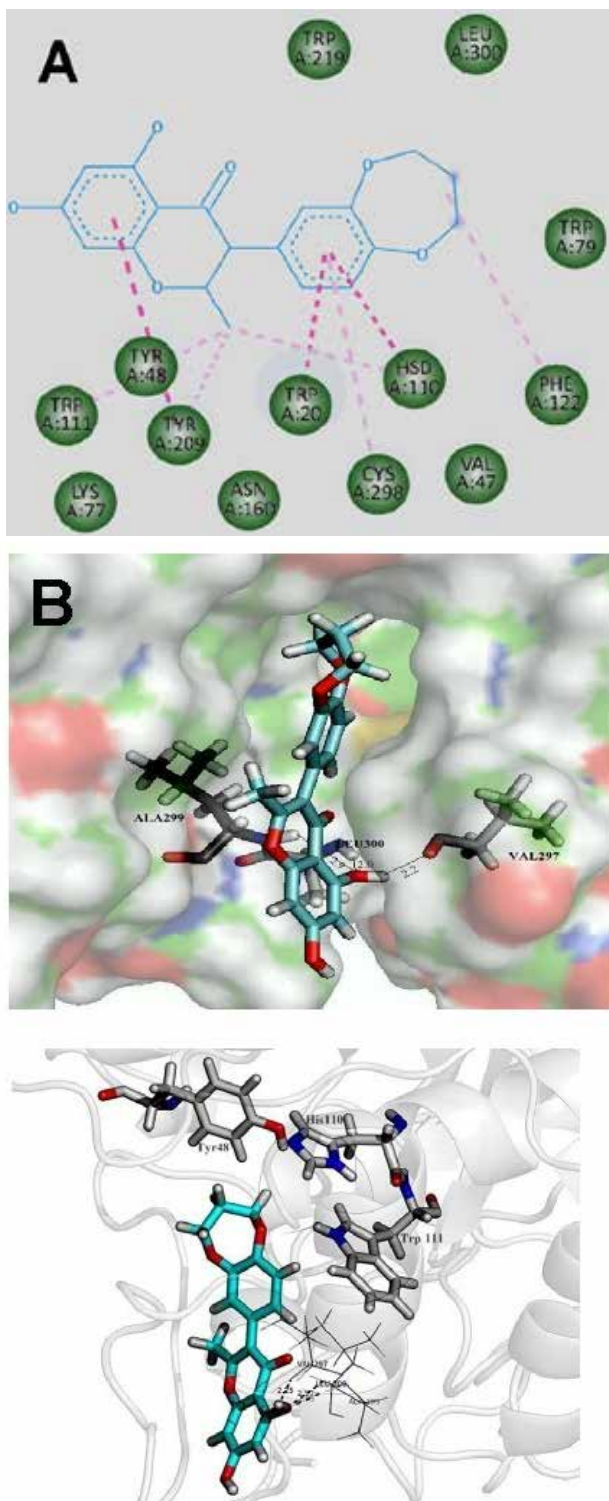


Fig. 10. 2D interaction for the hit molecule and aldose reductase (A). Different poses of hit molecule, occupying the specificity pocket (left) making interactions (left, right) with Val297, Ala299 and Leu300 at distances of 2.2Å, 2.9Å and 2.0Å respectively (B)

of -15.363 kcal/mol. It also did not interfere with the anionic region, as it docked into the active site entry region, which forms the pocket responsible for specificity. The molecule identified in this study effectively blocks glucose entry into the active site, covering almost the entire entry region while leaving a small space that prevents glucose from entering the anionic region. However, our final hit has a minor drawback: depending on its spatial orientation, it may or may not permit the entry of toxic aldehydes necessary for the detoxification mechanism.

Recent reports on the identification of thiazolidinone through docking showed interactions with residues Trp111, Ala299, Leu300 and Phe122 located at the specificity pocket, which also confirms our finding that the interactions with Trp111 is critical for the inhibition of aldose reductase. Toxicity prediction (Fig. 11) for the hit compounds using protoxII indicates that the compound is safe for oral consumption as it falls under category 5.

MD simulation of hit

Using the GROMACS molecular dynamics tool, a 100ns MD simulation of the final hit compound complexed with aldose reductase enzyme was performed. The stability and compactness of the protein structure were determined by standard protocols involving “root mean square deviation” (RMSD), “root mean square fluctuations” (RMSF), and “radius of gyration” (Rg). The average RMSD value is ~ 0.08 nm for the backbone protein (Fig. 12A). Higher RMSD values indicate that protein stability decreases, whereas a lower RMSD value indicates an increase in protein stability. RMSF calculates the fluctuations of individual residue in presence of the ligands.

The macromolecule-ligand complex was maintained in a triclinic box with dimensions of 43:54:47 and solvated using the Simple Point Charge (SPC) water model, neutralized with a 0.15 M NaCl salt concentration. The OPLS/AA force field was employed to parameterize the macromolecule and its ligands. Energy minimization was performed using the steepest descent technique to eliminate steric disturbances between the macromolecule and the ligand. The leapfrog and two-phase ensemble equilibration algorithms were utilized for integration in the NVT and NPT at fixed temperature (300 K) and pressure (1 bar). After initialization and equilibration, molecular dynamics simulations were conducted for 100 ns, with data collected to determine RMSD, RMSF, and hydrogen bonding.

The RMSD and RMSF for the hit-aldose reductase complex (Fig. 12B) showed an average RMSD of 0.1 nm during the period from 20 ns to 60 ns, indicating that the stability of the complex was

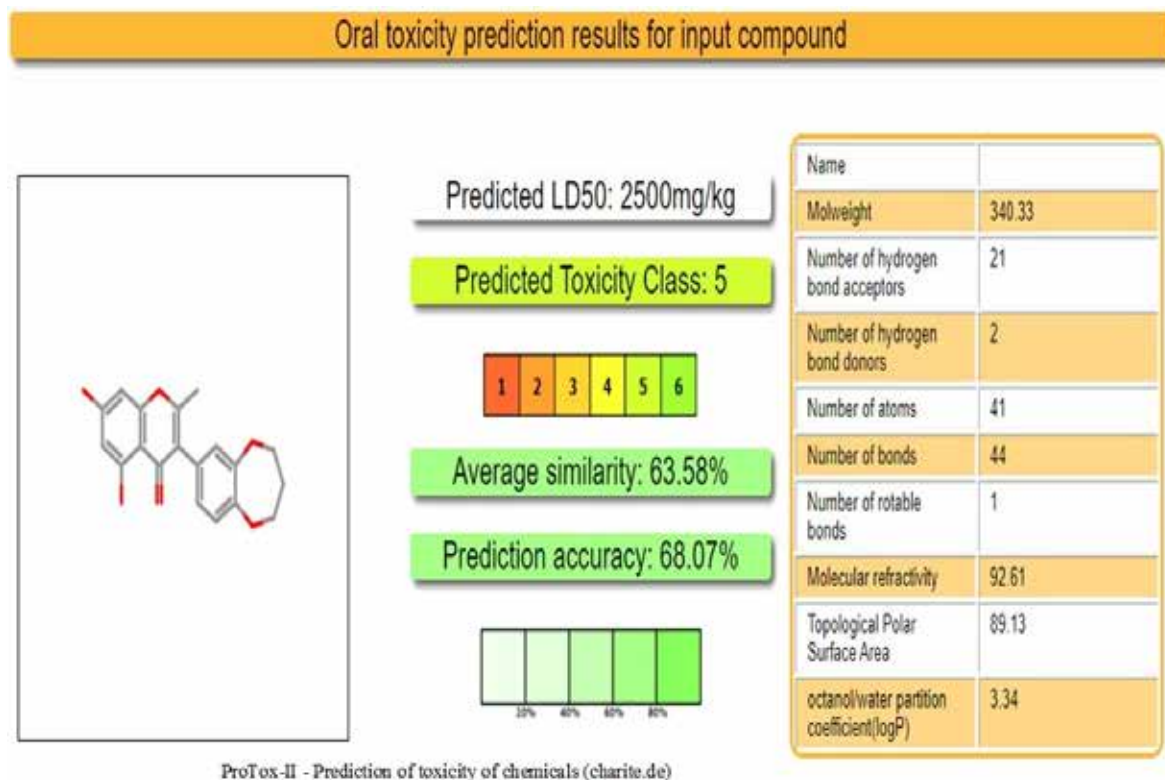


Fig. 11. Toxicity prediction for the hit molecule

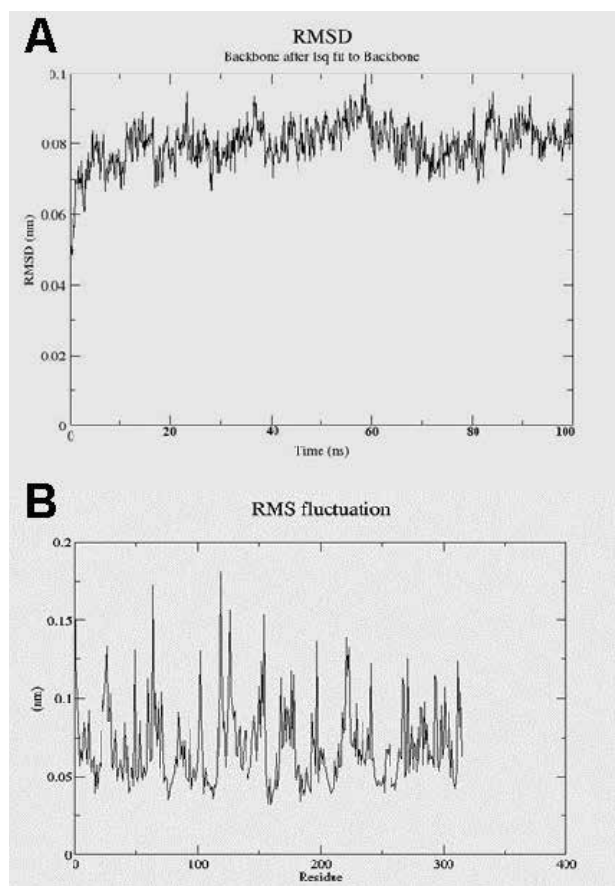


Fig. 12. RMSD of protein with hit compound (A). RMSF of protein with hit compound (B)

gradually maintained, with only slight deviations from the initial simulation (0.05 nm to 0.06 nm). The simulation results indicated that the complex remained stable from 25 ns to 100 ns, which is considered good stability throughout the simulation period. The RMSF analysis revealed an average fluctuation rate of 0.1 nm, confirming that the complex maintained structural stability with the ligand bound to it.

A study by Kondhare et al. (2022) describes the aldose reductase inhibitory activity of alkannin (Fig. 13), a naphthoquinone-based compound from plants in the Boraginaceae family. Docking studies showed that alkannin formed hydrogen bonds with Val297, Ala299, Leu300, and Ser302, along with hydrophobic interactions (Trp20, Val47,

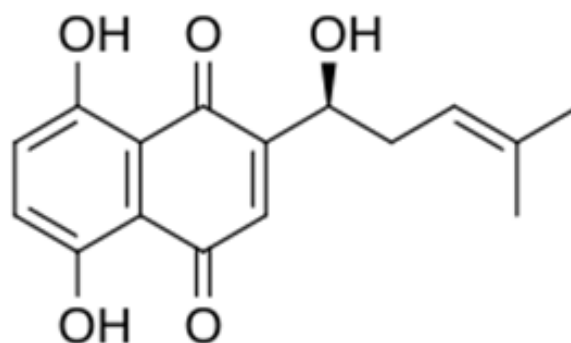


Fig. 13. Alkannin

Tyr48, Trp79, Trp111, Phe122, Trp219, Val297, Cys298, Ala299, Leu300, and Leu301). The results from *in vitro* studies show a potent dose-dependent inhibitory activity for aldose reductase at 22.77 μ M.

Given the recent emphasis on identifying effective aldose reductase inhibitors, our results represent a starting point for the extensive research needed to achieve this goal. Furthermore, the hit molecule identified here does not extend into the anionic region responsible for detoxifying toxic aldehydes produced by the lipid pathway. This is a crucial criterion for an aldose reductase inhibitor, as it prevents glucose from entering the active site. However, the binding orientation of this molecule may allow or restrict the entry of toxic aldehydes into the pocket. Specifically, it may permit the entry of methylglyoxal due to its size and volume, while it does not allow glyceraldehyde, a four-carbon linear molecule, to enter.

Conclusion

Molecular ligand docking into three regions - anionic region, specificity region, and active site region, allowed the identification of possible inhibitors that selectively bind to the specificity region. The hit molecule (mol_7921) bears much similarity to a flavonoid and can therefore be considered a good starting point for future studies. Unlike the other compounds that we analyzed and studied in our earlier workflow, this molecule (mol_7921, Fig. 9) does not extend into the anionic binding region or interfere with the residues Tyr48, His110, and Trp111, which are responsible for carrying out the detoxification mechanism of toxic aldehydes. This helped us fulfill the first objective of preventing glucose entry into the active site. However, close observations revealed that this molecule has bound in such a spatial orientation that it may or may not allow the entry of toxic aldehydes into the pocket. Methylglyoxal, being a four-carbon linear molecule, might find it difficult to enter, while glyceraldehyde may be allowed to enter the pocket due to its size and volume. This is due to the presence of a seven-membered ring at one end, which is responsible for this drawback. The results of the simulation showed the stability of the complex from 25 ns to 100 ns, indicating the intact nature of the bound form throughout the simulation period. The structural stability of the ligand-bound complex is further supported by RMSF, wherein the average fluctuation rate is 0.1 nm. However, the hit molecule needs to be tested to confirm the binding mode and its potential use for diabetic neuropathy.

Acknowledgements. The authors thank the Management of Karpagam Charities Trust, Coimbatore and SASTRA

University, Thanjavur for their support throughout all aspects of our study.

References

- Bakal, R.L., Jawarkar, R.D., Manwar, J.V., Jaiswal, M.S., Ghosh, A., Gandhi, A., Zaki, M.E., Al-Hussain, S., Samad, A., Masand, V.H., & Mukerjee, N. (2022).** Identification of potent aldose reductase inhibitors as antidiabetic (anti-hyperglycemic) agents using QSAR based virtual screening, molecular docking, MD simulation and MMGBSA approaches. *Saudi Pharmaceutical Journal*, 30(6), 693-710.
- Balestri, F., Moschini, R., Mura, U., Cappiello, M. & Del Corso, A. (2022).** In search of differential inhibitors of aldose reductase. *Biomolecules*, 12(4), 485.
- Chaudhry, P.S., Cabrera, J., Juliani, H.R., & Varma, S.D. (1983).** Inhibition of human lens aldose reductase by flavonoids, sulindac and indomethacin. *Biochemical Pharmacology*, 32(13), 1995-1998.
- Chen, C.Y., Zhang, J.Q., Li, L., Guo, M.M., He, Y.F., Dong, Y.M., Meng, H., & Yi, F. (2022).** Advanced glycation end products in the skin: Molecular mechanisms, methods of measurement, and inhibitory pathways. *Frontiers in Medicine*, 9, 837222.
- Ciccone, L., Petrarolo, G., Barsuglia, F., Fruchart-Gaillard, C., Cassar Lajeunesse, E., Adewumi, A.T., Soliman, M.E., La Motta, C., Orlandini, E., & Nencetti, S. (2022).** Nature-inspired o-benzyl oxime-based derivatives as new dual-acting agents targeting aldose reductase and oxidative stress. *Biomolecules*, 12(3), 448.
- Friesner, R.A., Murphy, R.B., Repasky, M.P., Frye, L.L., Greenwood, J.R., Halgren, T.A., Sanschagrin, P.C., & Mainz, D.T. (2006).** Extra precision glide: Docking and scoring incorporating a model of hydrophobic enclosure for protein–ligand complexes. *Journal of medicinal chemistry*, 49(21), 6177-6196.
- Goto, Y., Hotta, N., Shigeta, Y., Sakamoto, N. and Kikkawa, R. (1995).** Effects of an aldose reductase inhibitor, epalrestat, on diabetic neuropathy. Clinical benefit and indication for the drug assessed from the results of a placebo-controlled double-blind study. *Biomedicine & Pharmacotherapy*, 49(6), 269-277.
- Gronda, E., Jessup, M., Iacoviello, M., Palazzuoli, A., & Napoli, C. (2020).** Glucose metabolism in the kidney: neurohormonal activation and heart failure development. *Journal of the American Heart Association*, 9(23), e018889.

- Imran, A., Shehzad, M.T., Shah, S.J.A., Al Adhami, T., Laws, M., Rahman, K.M., Alharthy, R.D., Khan, I.A., Shafiq, Z., & Iqbal, J. (2022). Development and exploration of novel substituted thiosemicarbazones as inhibitors of aldose reductase via *in vitro* analysis and computational study. *Scientific Reports*, 12(1), 5734.
- Jensen, T.S., Karlsson, P., Gylfadottir, S.S., Andersen, S.T., Bennett, D.L., Tankisi, H., Finnerup, N.B., Terkelsen, A.J., Khan, K., Themistocleous, A.C., & Kristensen, A.G. (2021). Painful and non-painful diabetic neuropathy, diagnostic challenges and implications for future management. *Brain*, 144(6), 1632-1645.
- Klebe, G., Krämer, O., & Sotriffer, C. (2004). Strategies for the design of inhibitors of aldose reductase, an enzyme showing pronounced induced-fit adaptations. *Cellular and Molecular Life Sciences CMLS*, 61, 783-793.
- Kondhare, D. & Lade, H. (2017). Phytochemical profile, aldose reductase inhibitory, and antioxidant activities of Indian traditional medicinal *Coccinia grandis* (L.) fruit extract. *3 Biotech*, 7(6), 378.
- Kumar, H., Shah, A., & Sobhia, M.E. (2012). Novel insights into the structural requirements for the design of selective and specific aldose reductase inhibitors. *Journal of molecular modeling*, 18, 1791-1799.
- Madić, V., Jovanović, J., Stojilković, A., & Vasiljević, P. (2017). Evaluation of cytotoxicity of 'anti-diabetic'herbal preparation and five medicinal plants: an *Allium cepa* assay. *Biologica Nyssana*, 8(2), 151-158.
- Rajeswari, M., Santhi, N., & Bhuvaneshwari, V. (2014). Pharmacophore and virtual screening of JAK3 inhibitors. *Bioinformation*, 10(3), 157.
- Saeed, M., Tasleem, M., Shoib, A., Kausar, M.A., Sulieman, A.M.E., Alabdallah, N.M., El Asmar, Z., Abdelgadir, A., Al-Shammery, A., Alam, M.J., & Badroui, R. (2022). Identification of putative plant-based ALR-2 inhibitors to treat diabetic peripheral neuropathy. *Current Issues in Molecular Biology*, 44(7), 2825-2841.
- Singh, M., Kapoor, A., & Bhatnagar, A. (2021). Physiological and pathological roles of aldose reductase. *Metabolites*, 11(10), p.655.
- Sulaiman, A.H., Ghassan, Z.I., & Omar, T.N. (2022). Biochemical evaluation of carbonic anhydrase and some antioxidant markers in patients with diabetes complications. *Archives of Razi Institute*, 77(1), 169-178.
- Twarda-Clapa, A., Olczak, A., Bialkowska, A.M., & Koziolkiewicz, M. (2022). Advanced glycation end-products (AGEs): Formation, chemistry, classification, receptors, and diseases related to AGEs. *Cells*, 11(8), 1312.
- Verma, S.K. & Thareja, S. (2020). An overview on chemistry of natural aldose reductase inhibitors for the management of diabetic complications. *Studies in Natural Products Chemistry*, 65, 381-429.
- Yagihashi, S., Mizukami, H., & Sugimoto, K. (2011). Mechanism of diabetic neuropathy: where are we now and where to go?. *Journal of Diabetes Investigation*, 2(1), 18-32.
- Zhang, K., Lu, W.C., Zhang, M., Zhang, Q., Xian, P.P., Liu, F.F., Chen, Z.Y., Kim, C.S., Wu, S.X., Tao, H.R., & Wang, Y.Z. (2022). Reducing host aldose reductase activity promotes neuronal differentiation of transplanted neural stem cells at spinal cord injury sites and facilitates locomotion recovery. *Neural Regeneration Research*, 17(8), 1814-1820.
- Zheng, Q., Li, S., Li, X., & Liu, R. (2021). Advances in the study of emodin: an update on pharmacological properties and mechanistic basis. *Chinese Medicine*, 16, 1-24.
- Zhu, J., Qi, G., Kuang, Y., Zhao, Y., Sun, X., Zhu, C., Hao, X., & Han, Z. (2022). Identification of 9H-purin-6-amine derivatives as novel aldose reductase inhibitors for the treatment of diabetic complications. *Archiv der Pharmazie*, 355(8), 2200043.

